Amino Acids (2016) 48:1209–1220
DOI 10.1007/s00726-015-2156-1

ORIGINAL ARTICLE

Characterization of aromatic aminotransferases from *Ephedra sinica* Stapf

Korey Kilpatrick[1,2] · Agnieszka Pajak[2] · Jillian M. Hagel[3] · Mark W. Sumarah[2] · Efraim Lewinsohn[4] · Peter J. Facchini[3] · Frédéric Marsolais[1,2]

Received: 9 June 2015 / Accepted: 13 December 2015 / Published online: 1 February 2016

Abstract *Ephedra sinica* Stapf (Ephedraceae) is a broom-like shrub cultivated in arid regions of China, Korea and Japan. This plant accumulates large amounts of the ephedrine alkaloids in its aerial tissues. These analogs of amphetamine mimic the actions of adrenaline and stimulate the sympathetic nervous system. While much is known about their pharmacological properties, the mechanisms by which they are synthesized remain largely unknown. A functional genomics platform was established to investigate their biosynthesis. Candidate enzymes were obtained from an expressed sequence tag collection based on similarity to characterized enzymes with similar functions. Two aromatic aminotransferases, EsAroAT1 and EsAroAT2, were characterized. The results of quantitative reverse transcription-polymerase chain reaction indicated that both genes are expressed in young stem tissue, where ephedrine alkaloids are synthesized, and in mature stem tissue. Nickel affinity-purified recombinant EsAroAT1 exhibited higher catalytic activity and was more homogeneous than EsAroAT2 as determined by size-exclusion chromatography. EsAroAT1 was highly active as a tyrosine aminotransferase with α-ketoglutarate followed by α-ketomethylthiobutyrate and very low activity with phenylpyruvate. In the reverse direction, catalytic efficiency was similar for the formation of all three aromatic amino acids using L-glutamate. Neither enzyme accepted putative intermediates in the ephedrine alkaloid biosynthetic pathway, *S*-phenylacetylcarbinol or 1-phenylpropane-1,2-dione, as substrates.

Keywords *Ephedra sinensis* Stapf Ephedraceae · Aminotransferase · Aromatic amino acids · L-Tyrosine · Pyridoxal 5′-phosphate · Transcriptome analysis

Handling Editor: F. Hollfelder.

Electronic supplementary material The online version of this article (doi:10.1007/s00726-015-2156-1) contains supplementary material, which is available to authorized users.

✉ Frédéric Marsolais
Frederic.Marsolais@agr.gc.ca

[1] Department of Biology, University of Western Ontario, London, ON N6A 5B7, Canada

[2] Agriculture and Agri-Food Canada, Genomics and Biotechnology, London Research and Development Centre, 1391 Sandford St., London, ON N5V 4T3, Canada

[3] Department of Biological Sciences, University of Calgary, Calgary, AB, Canada

[4] Department of Aromatic, Medicinal and Spice Crops, Newe Ya'ar Research Center, Agricultural Research Organization, 30095 Ramat Yishay, Israel

Introduction

Ephedra sinica Stapf (Ephedraceae) is a perennial, broom-like shrub cultivated in arid regions of China, Korea and Japan (Bensky et al. 1986). This traditional Chinese medicinal plant has been utilized by humans for over 5000 years. *Ma Huang*, a tea containing dried *E. sinica* stems was utilized for the treatment of asthma, fever, coughs and lack of sweating, and to promote urination and reduce edema (Bensky et al. 1986; Bruneton 1995). All aerial tissues of this plant accumulate the ephedrine alkaloids, with the stems accumulating the highest amounts, up to 3 % of dry weight (Krizevski et al. 2010).

The ephedrine alkaloids are a class of phenylpropylamino alkaloids which are analogs of amphetamine. As such they act as adrenergic agonists, mimicking the actions of adrenaline by direct agonist activity and indirect release of norepinephrine (Bruneton 1995; Rothman et al. 2003).

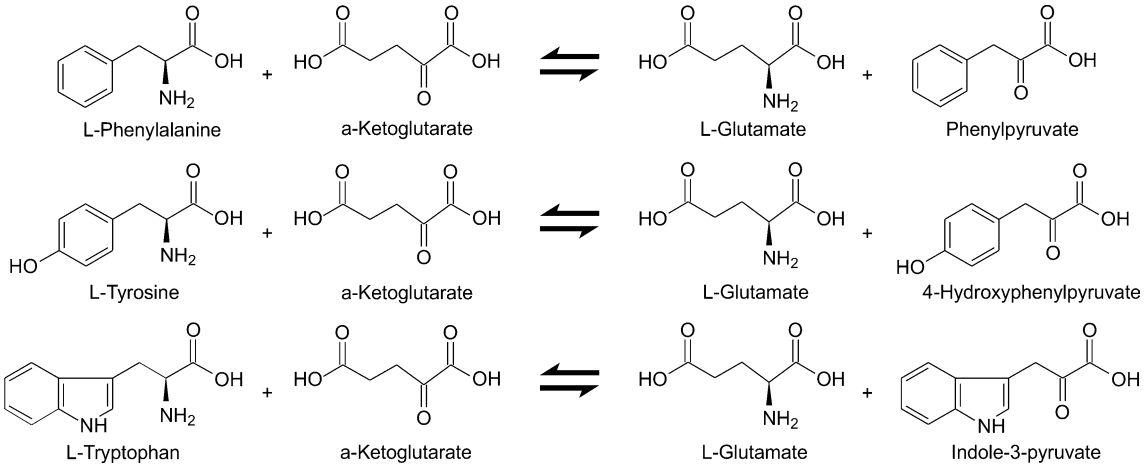

Fig. 1 Reactions catalyzed by *E. sinica* aromatic aminotransferases

These pharmacoactive stimulants, including (*S*)-cathinone, (*1S*,*2S*)-norpseudoephedrine, (*1R*,*2S*)-norephedrine, (*1S*,*2S*)-pseudoephedrine and (*1R*,*2S*)-ephedrine are collectively known as the ephedrine alkaloids. (*1R*,*2S*)-Norephedrine and (*1R*,*2S*)-ephedrine are used to treat acute asthma attacks, rhinitis and sinusitis because of their vasoconstrictive properties (Bruneton 1995). (*1R*,*2S*)-Ephedrine is also used to counteract anesthesia and overdoses of depressant drugs as well as treatment for bronchial asthma and various allergies (Lewis and Elvin-Lewis 1977). (*1S*,*2S*)-Pseudoephedrine is a widely used nasal decongestant (Bruneton 1995). (*1R*,*2S*)-Ephedrine is used as a controversial and risky weight-loss or exercise supplement and a number of deaths have been attributed to its use (Haller and Benowitz 2000). While much is known about the pharmacological properties of these stimulants, the biological mechanisms by which they are synthesized remain largely unknown.

The proposed biosynthetic pathway for production of the ephedrine alkaloids can be found in recently published articles by Hagel et al. (2012) and Krizevski et al. (2012). Early radiolabelling experiments using *Catha edulis* (a taxonomically unrelated plant species which also produces the ephedrine alkaloids) determined that L-phenylalanine (see Fig. 1) is the initial precursor of the ephedrine alkaloids (Leete 1958). Those findings were later confirmed using *Ephedra distachya* stems (Yamasaki et al. 1969). So far, only the step catalyzed by phenylalanine ammonia lyase has been characterized at the molecular level in *E. sinica* (Okada et al. 2008). An aromatic aminotransferase could catalyze the formation of phenylpyruvate from L-phenylalanine as a precursor to benzaldehyde (Hagel et al. 2011), a pathway occurring in bacteria (Nierop Groot and de Bont 1999). Benzaldehyde might then be condensed with pyruvate by a benzaldehyde carboxyligase to form the ephedrine alkaloid precursors (*R*)-phenylacetylcarbinol, (*S*)-phenylacetylcarbinol, (*R*)-2-hydroxypropiophenone, (*S*)-2-hydroxypropiophenone and 1-phenylpropane-1,2-dione (Krizevski et al. 2012). Beside the provision of precursors for the ephedrine biosynthetic pathway, aminotransferases may also be involved in the formation of the intermediate (*S*)-cathinone from 1-phenylpropane-1,2-dione (Hagel et al. 2012; Grue-Sørensen and Spenser 1994).

Aminotransferases (EC 2.6.1) are enzymes that catalyze the reversible transfer of an amino group from an amino donor, typically an amino acid, to the carbonyl group of an amino acceptor, typically a keto acid. They are involved in a number of essential biological processes including anabolism and catabolism of amino acids, nitrogen assimilation, vitamin biosynthesis, plant stress responses and secondary metabolism (Givan 1980; Liepman and Olsen 2004). Aminotransferases are part of the pyridoxal-5′-phosphate dependent class of enzymes. Pyridoxal-5′-phosphate is covalently bound through an imine linkage to the ε-amino group of the conserved lysine residue in the active site of the enzyme (Mehta et al. 1993). Most aminotransferases are able to accept multiple substrates, given the usually reversible nature of the reaction, and employ a ping–pong reaction mechanism (Hirotsu et al. 2005). Among the seven fold types of pyridoxal-5′-phosphate-dependent enzymes, aminotransferases belong to types I and IV (Schneider et al. 2000). There are six subfamilies of aminotransferases defined by a different Pfam domain (Finn et al. 2014; Rudat et al. 2012), five of which belong to fold-type I. Representatives of subfamilies I and II are aspartate and aromatic aminotransferases. ω-Aminotransferases belong to subfamily III, and phosphoserine aminotransferase to subfamily V. D-Alanine and branched chain amino acid aminotransferases belong to subfamily IV and to fold-type IV.

To investigate ephedrine alkaloid biosynthesis, a snapshot of the *E. sinica* stem transcriptome was generated by

next-generation sequencing of RNA extracted from young stem tissue. The data were assembled and annotated to create a functional genomics platform which was triaged for candidate biosynthetic genes. This information was used to identify and characterize two aromatic aminotransferases.

Materials and methods

Plant material

E. sinica Stapf seeds were purchased from Horizon Herbs (Williams, OR) and Richters Herbs (Goodwood, ON). Seeds were sown in the spring and fall months in 50 % sand, 50 % cactus soil mixture and grown in a greenhouse with at least 14 h of light per day. Supplemental 220 V, high-pressure sodium light and 20:20:20 (nitrogen–phosphorus–potassium) fertilizer was used. 'Young' *E. sinica* tissues used in this study were the freshly grown tips of the stems and light green in color. 'Mature' tissues were the lower portions of stems and dark green in colour. After sample collection, fresh plant material was immediately frozen in liquid nitrogen and stored at −80 °C until use.

RNA extraction from *E. sinica* stem tissue

Total RNA was extracted from *E. sinica* stems following a modified protocol for extracting RNA from tissues containing high levels of procyanidins (Wang and Vodkin 1994). Approximately 500 mg of ground stem tissue was used in place of 50 mg of lyophilized seed coats. After washing with 2 M LiCl, the RNA pellet was resuspended in 100 µl of diethylpyrocarbonate-treated water. Then, 10 µl of 3 M NaOAc (pH 5.2) and 300 µl of 95 % (v/v) ethanol was added and the solution was placed at −20 °C overnight. The pellet was collected by centrifugation (25,000×*g* for 20 min at 4 °C) and washed twice with 70 % (v/v) ethanol. The RNA pellet was dried, resuspended in diethylpyrocarbonate water and stored at −80 °C until use.

Next-generation sequencing

A sample of total RNA (10 µl at 2.3 µg/µl) extracted from young *E. sinica* stems was sent for next-generation sequencing on the Illumina HiSeq 2000 RNA-seq platform (single channel, 100 base pair, paired-end reads). The sequencing was performed as per the manufacturers' specifications at the McGill University and Génome Québec Innovation Centre. Expressed sequence tag data from the library were assembled using the Velvet algorithms for de novo short read assembly (Zerbino and Birney 2008) and deposited in the MAGPIE (automated genomics project investigation environment) portal (Groves et al. 2015). These data were mined for candidate aminotransferase genes in the ephedrine alkaloid biosynthetic pathway based on sequence similarity to previously characterized aromatic aminotransferases.

RT-PCR and cloning of *E. sinica* aromatic aminotransferases

E. sinica RNA was treated with DNaseI (RNase-free) (Life Technologies, Burlington, ON) following manufacturers' guidelines to remove any residual DNA. The RNA was reverse transcribed into cDNA using qScript cDNA SuperMix (Quanta BioSciences, Gaithersburg, MD) following manufacturers' guidelines and stored at −20 °C until use. PCR primers used to amplify the open reading frames examined in this study were as follows: forward (5′-CTACGGATCCATGGCAAGCAATGGGGAATGG-3′) and reverse (5′-CTACGGATCCATGGCAAGCAATGGGGAATGG-3′) for *EsAroAT1* and forward (5′-CTACGGATCCATGGTGAAGTGGAATTTTAAGCCAAGC-3′) and reverse (5′-CTACAAGCTTCTATAAACTCCTATAATGTCTGCGACAGAATGC-3′) for *EsAroAT2*. Restriction enzyme sites for *Bam*HI (forward) and *Kpn*I (reverse) are underlined. *Pfx50* DNA polymerase (Life Technologies) was used and the PCR reaction consisted of denaturing at 94 °C for 2 min, 35 cycles of 94 °C for 15 s, 60.5 °C for 30 s and 68 °C for 90 s, and a final extension at 68 °C for 5 min. PCR products were cloned into pCR4Blunt-TOPO vector and sequenced with a 3130 XL Genetic Analyzer (Life Technologies). The candidate cDNAs were subcloned into the pQE30 expression vector (Qiagen, Toronto, ON) by restriction enzyme-mediated cloning using *Bam*HI and *Kpn*I (*EsAroAT1*) or *Bam*HI and *Hin*dIII (*EsAroAT2*) restriction endonucleases (New England Biolabs, Whitby, ON) and T4 DNA ligase (Life Technologies) following manufacturers' guidelines. *E. coli* strain XL10-Gold (Agilent Technologies, Mississauga, ON) was used for cloning and expression of candidate cDNAs.

RT-quantitative PCR

E. sinica RNA was extracted in triplicate from both young and mature stem tissue and cDNA was generated as described above to determine relative gene expression levels of *EsAroAT1* and *EsAroAT2*, compared to the elongation factor 1-alpha (*Ef1α*) reference gene. PCR primers used in RT-quantitative PCR analysis were as follows: forward (5′-GCTCTCCTTGCTTTCACCCT-3′) and reverse (5′-TGGGATTTTGTCGGGGTTGT-3′) for *Ef1α* (159 bp amplicon); forward (5′-TGACAGTTGGATGCTCTCAGG-3′) and reverse (5′-CCTTCCACTCATCCTCTGGG-3′) for *EsAroAT1* (174 bp amplicon); and forward (5′-GCAGGCAAGAAGAGCTGTTTC-3′) and

reverse (5′-ACAAGGCTTCATACTGTGGGT-3′) for *EsAroAT2* (184 bp amplicon). cDNA was diluted eightfold and 2 µl was amplified with 5 µl of SsoFast EvaGreen Supermix in a final volume of 10 µl using a CFX96 Real-Time Detection System (Bio-Rad, Mississauga, ON). Reactions were carried out in hard-shell 96-well clear PCR plates. Controls without template were performed in triplicate in each plate. Reactions were performed in triplicate and contained primers at a concentration of 0.5 µM for *EsAroAT1* and *EsAroAT2*, and 0.48 µM for *Ef1α*. The PCR program consisted of an initial step of 95 °C for 3 min followed by 35 cycles of 95 °C for 10 s and 59.5 °C for 30 s. Data were analyzed with the CFX Manager 2.0 software and expressed as the cycle number required to reach a threshold fluorescence value (C_t). Data were normalized to the mean C_t of the reference gene *Ef1α*, for which variation between samples was ≤0.7. Melt curve analysis was used to confirm the specificity of each primer pair in comparison with no template controls. Efficiency of PCR reactions was calculated from a standard curve of C_t versus the logarithm of starting template quantity. Each assay was optimized so that the efficiency ranged between 100 and 113 %, with a coefficient of determination (R^2) ≥ 0.99.

Expression and purification of *E. sinica* aromatic aminotransferases

Fresh overnight culture containing recombinant plasmid were grown in LB media and used to inoculate 500 ml of NZY media containing 100 µg/ml of ampicillin. Cultures were incubated at 37 °C until an OD_{600} of ~0.6 was reached. Expression of His-tagged candidate aminotransferases was induced by the addition of 1 mM isopropyl β-D-1-thiogalactopyranoside and cells were cultured overnight (18 h) at room temperature (~21 °C). Cells were collected by centrifugation (5500×*g* for 5 min at 4 °C) and frozen at −20 °C to enhance lysis. After native lysis buffer (50 mM sodium phosphate monobasic, 300 mM sodium chloride and 10 mM imidazole at pH 8.0) was used to resuspend cells, 1 mg/ml lysozyme was added and lysates were placed on ice for 30 min. French Press and sonication were used to further lyse cells. After centrifugation to pellet cell debris (15,500×*g* for 45 min at 4 °C), Ni–NTA agarose beads (Qiagen) were added and the solutions were incubated at 4 °C for 2 h on a slow rotor. The Ni–NTA protein solutions were centrifuged (3500×*g* for 3 min at 4 °C) and the supernatant discarded. Pellets were washed ten times with native wash buffer (50 mM sodium phosphate monobasic, 300 mM sodium chloride and 40 mM imidazole at pH 8.0) to remove weakly bound proteins. Recombinant proteins were eluted from the Ni–NTA agarose by the addition of native elution buffer (50 mM sodium phosphate monobasic, 300 mM sodium chloride and 250 mM imidazole at pH 8.0). Buffer exchange was performed using PD-10 columns (GE Healthcare Life Sciences, Baie d'Urfé, QC) following the manufacturers' protocol. Recombinant proteins were concentrated using an Amicon Ultra-4 filter (EMD Millipore Corporation, Billerica, MA) and stored at −80 °C in 100 mM HEPES buffer (pH 8.2) with 1 mM sodium EDTA and 20 % (v/v) glycerol. Eluted proteins were further purified using size-exclusion chromatography on a HiLoad Superdex 200 prep grade column with 20 mM Tris buffer, pH 7.5, 150 mM sodium chloride on an ÄKTApurifier system (GE Healthcare Life Sciences). Molecular mass of the eluted protein was calculated by generating a standard curve of k_{av} versus the logarithm of the molecular weight of several protein standards, where k_{av} = elution volume − void volume/column volume − void volume. Protein concentration was determined using the Bio-Rad protein assay solution with bovine serum albumin as standard. SDS-PAGE was performed and gels stained with Coomassie Brilliant Blue R250 stain to confirm that the proper protein had been purified by comparison of the empirical and predicted molecular mass.

Absorption spectroscopy of EsAroAT proteins

Absorption spectra of purified recombinant proteins were determined using a DU 600 spectrophotometer (Beckman Coulter, Mississauga, ON). The typical wavelength scan was between 250 and 600 nm and used 0.5 mg/ml of purified protein in 25 mM HEPES buffer with 100 mM sodium chloride (pH 7.5).

Enzyme assays

Enzyme kinetics for the aromatic aminotransferase reactions were determined by monitoring the absorbance of reaction products by spectrophotometry as previously described (Collier and Kohlhaw 1972). Prior to kinetic analysis, the enzymatic reactions described herein were standardized by ensuring linear product formation at 10, 20, 30, 40, 50 and up to 60 min. Production of 4-hydroxyphenylpyruvate was monitored at 331 nm (ε_{331} = 19,920 M^{-1} cm^{-1}), phenylpyruvate at 320 nm (ε_{320} = 17,500 M^{-1} cm^{-1}) and indole-3-pyruvate at 328 nm (ε_{328} = 10,000 M^{-1} cm^{-1}). The assay contained 100 mM Tris–HCl buffer (pH 9.0), 0.1 µg recombinant protein (0.01 µg for L-tyrosine), 0.1 mM sodium EDTA and the following substrate concentrations: 0.3–6 mM amino group donor (L-tyrosine, L-phenylalanine or L-tryptophan) and 0.1–1.5 mM amino group acceptor (α-ketoglutarate) in a total volume of 250 µl. Reactions were incubated at 30 °C for 30 min, terminated by the addition of 70 µl of 2 N NaOH and placed at room temperature for an additional 30 min before scanning, except for phenylpyruvate

which was scanned immediately. When required, pyridoxal 5′-phosphate was added at a concentration of 0.1 mM.

Enzyme kinetics for the aromatic aminotransferase reactions with L-glutamate were determined by coupling with α-ketoglutarate dehydrogenase and monitoring the absorbance of NADH at 340 nm (ε_{340} = 6300 M^{-1} cm^{-1}), as previously described (Prabhu and Hudson 2010). Prior to kinetic analysis, the reverse reaction was monitored continuously—at 3 min intervals between 3 and 30 min—and demonstrated linear NADH formation for up to 30 min. The 500 µl assay contained 100 mM Tris–HCl buffer (pH 9.0), 2 µg recombinant protein, 0.1 mM sodium EDTA, 600 mg α-ketoglutarate dehydrogenase (0.28 U/mg), 0.3 mM coenzyme A, 0.3 mM NAD^+ and the following substrate concentrations: 0.3–25 mM amino group donor (L-glutamate) and 0.05–0.9 mM 4-hydroxyphenylpyruvate, 0.05–0.9 mM phenylpyruvate or 0.01–0.3 mM indole-3-pyruvate. Reactions were incubated at 30 °C for 30 min then immediately transferred to Greiner Bio One UV-Star 96-well, flat bottom plates (Monroe, NC) and scanned using a Bio-Tek PowerWave XS plate reader (Winooski, VT). Enzymatic assays excluding recombinant enzyme, excluding a substrate and using heat-inactivated enzyme were used as negative controls. Beer's Law was used to determine concentrations of the reaction products. Apparent V_{max} and K_m values were calculated using Lineweaver–Burk (double reciprocal) plots for analysis of the Michaelis–Menten equation.

Catalytic activity with 1,2-phenylpropanedione or (*S*)-phenylacetylcarbinol was monitored in a similar way using L-glutamate as amino group donor by coupling with α-ketoglutarate dehydrogenase. Concentration of acceptor substrate ranged between 0.01 and 1.0 mM. (*S*)-Phenylacetylcarbinol was purchased from Toronto Research Chemicals (North York, Ontario, Canada) as an 80 % enantiomeric excess mixture. Catalytic activity with 1,2-phenylpropanedione or (*S*)-phenylacetylcarbinol was also screened with a mixture of amino acids as potential amino group donors (Amino Acid Standard H) (Thermo Fisher Scientific, Burlington, Ontario, Canada). Transamination of 1,2-phenylpropanedione or (*S*)-phenylacetylcarbinol was monitored by GC–MS as described by Krizevski et al. (2010, 2012).

Results

Next-generation sequencing and annotated *E. sinica* expressed sequence tag library

E. sinica cDNA was generated and sequenced using the Illumina HiSeq 2000 platform at the McGill University and Génome Québec Innovation Centre. This high-throughput sequencing method generated more than 95 million, 100 bp, paired-end reads. The collection of data were assembled and annotated by Dr. Christoph Sensen's laboratory at the University of Calgary. The assembly yielded 59,448 contigs spanning 89 million nucleotide bases (Groves et al. 2015). This annotated expressed sequence tag database was triaged to select candidate biosynthetic enzymes involved in production of the ephedrine alkaloids.

Aromatic aminotransferase candidates

When blast searched with the deduced amino acid sequences of prephenate aminotransferase from petunia, aromatic aminotransferases from melon and rose, and tyrosine aminotransferase from opium poppy (Maeda et al. 2011; Gonda et al. 2010; Hirata et al. 2012; Lee and Facchini 2011; Dal Cin et al. 2011; de la Torre et al. 2006, 2014; Graindorge et al. 2010), there were nine candidate contigs encoding aromatic aminotransferases that putatively catalyze reactions involving aromatic substrates identified in the expressed sequence tag database (ranging between 5×10^{-17} and 0 in *e* value). Two were annotated as prephenate aromatic aminotransferases, and the remaining seven were annotated as aromatic or tyrosine aminotransferases. Arabidopsis also has seven annotated tyrosine aminotransferases (Prabhu and Hudson 2010). RT-PCR was used to generate cDNAs for each candidate, which were cloned into expression vectors and expressed in *Escherichia coli.* Two of the candidates, EsAroAT1 and EsAroAT2 (encoded by contigs 13244 and 12701, respectively) were found to have activity with L-phenylalanine, L-tyrosine and L-tryptophan (Fig. 1) and were selected for further characterization. A comparison of their deduced amino acid sequences with aromatic aminotransferases from various organisms is summarized in Table 1. A similar level of sequence identity of ca. 46 % was observed between EsAroAT1 and the other plant aromatic aminotransferases. There is often less than 50 % identity when comparing aromatic aminotransferases within a species or between different plant species (Prabhu and Hudson 2010). An alignment of the deduced amino acid sequences revealed the presence of several conserved amino acid residues, including the invariant lysine which forms a covalent intermediate with the co-factor, pyridoxal 5′-phosphate (Online Resource 1).

Gene expression analysis of EsAroAT1

Relative gene expression levels of *EsAroAT1* and *EsAroAT2* were determined by RT-quantitative PCR and comparison of their transcript levels to the elongation factor 1-alpha (*Ef1α*) reference gene in young and mature *E. sinica* stem tissue (Table 2). *EsAroAT1* expression was similar between those two developmental stages, whereas *EsAroAT2* expression was lower in mature stem as compared with young stem by ca. fivefold.

Table 1 Identity in deduced amino acid sequence of EsAroAT2 and previously characterized aromatic aminotransferase enzymes from plants and *E. coli* to EsAroAT1

Accession	Annotation	Organism	Percent identity to EsAroAT1[a]
KC438923	Aromatic AT[b]	*Ephedra sinica*	46
KC954706.1	Ab-ArAT4	*Atropa belladonna*	48
AB669189.1	Phenylalanine AT	*Rosa 'Yves Piaget'*	47
KF511589.1	Phenylpyruvate AT	*Petunia hybrida*	47
AT5G36160	Tyrosine AT	*Arabidopsis thaliana*	46
AT5G53970	TAT7	*Arabidopsis thaliana*	46
ADC45389.1	Aromatic AT	*Cucumis melo*	45
ADC33123.1	Tyrosine AT	*Papaver somniferum*	44
AAA24703.1	Tyrosine AT	*Escherichia coli*	20

[a] Genbank accession number KC438292

[b] *AT* aminotransferase

Table 2 Normalized gene expression level of *EsAroAT1* and *EsAroAT2* as determined by RT-quantitative PCR relative to *Ef1α*. Average C_t value is in parenthesis

	Young stem	Mature stem	*t* test *p* value
EsAroAT1	1.30 ± 0.10 (22.4)	1.02 ± 0.18 (22.1)	n. s.
EsAroAT2	1.47 ± 0.28 (23.8)	0.29 ± 0.06 (25.4)	0.002
t test *p* value	n.s.	0.002	

Physical characteristics of recombinant EsAroAT enzymes

The predicted molecular mass of EsAroAT1 is 45 and 46 kDa, respectively. Figure 2a shows an SDS-PAGE of nickel affinity-purified recombinant EsAroAT1 and EsAroAT2. These preparations were used to acquire absorption spectra (Fig. 2b). The spectrum of EsAroAT1 had a peak at approximately 430 nm, a characteristic of bound pyridoxal 5′-phosphate (Ishikawa et al. 1996). The spectrum of EsAroAT2 did not have a peak in the 400 nm range indicating that pyridoxal 5′-phosphate was not present. These results confirmed visual observations that purified EsAroAT1 was yellowish-green in colour, suggesting that pyridoxal 5′-phosphate was bound to the enzyme. Similar observations were reported for Arabidopsis tyrosine aminotransferase At5g36160 (Prabhu and Hudson 2010). The molecular masses of native EsAroAT1 and EsAroAT2, as determined by size-exclusion chromatography, were 75 and 71 kDa, respectively (Fig. 2c–e). These data confirmed that EsAroAT1 and EsAroAT2 occur as homodimers, as expected for aminotransferases. The EsAroAT2 preparation was not as homogeneous as that of EsAroAT1 as demonstrated by the presence of three distinct peaks in the chromatogram. These correspond to the monomeric form (ca. 42 kDa), the homodimer, and most likely a heterodimer (ca. 117 kDa) formed with the chaperone DnaK, a host protein of ca. 68 kDa commonly co-purified with recombinant proteins from *E. coli* (Bolanos-Garcia and Davies 2006; Howell et al. 2006). This conclusion is supported by the observation of a protein band of ca. 70 kDa in the corresponding size-exclusion fraction.

Consistent with the visual observations and absorption spectra, EsAroAT1 did not require exogenously added pyridoxal 5′-phosphate for aromatic aminotransferase activity but EsAroAT2 did. Both EsAroAT1 and EsAroAT2 exhibited tyrosine and phenylalanine aminotransferase activity in initial enzymatic assays. However, the specific activity of EsAroAT1 was ca. threefold higher than that of EsAroAT2 when using tyrosine as amino donor and ca. sevenfold higher when using phenylalanine as donor (specific activities of EsAroAT1 were equal to 7 and 2.1 nkatal mg^{-1}, respectively). Neither EsAroAT1, EsAroAT2, nor the remaining five candidate aromatic aminotransferases were found to transaminate the intermediates of ephedrine alkaloid biosynthesis, 1-phenylpropane-1,2-dione or *S*-phenylacetylcarbinol when tested with L-glutamate, or a mixture of proteinogenic amino acids as amino group donors. Due to the lack of homogeneity of EsAroAT2, kinetic properties were only characterized for EsAroAT1.

Kinetic characterization of EsAroAT1

After optimizing the temperature (30 °C), duration (30 min) and amount of recombinant EsAroAT1 enzyme used (0.01–0.1 μg) the optimum pH was determined for the forward tyrosine aminotransferase reaction (Fig. 3a). There appeared to be two values of pH optima, of 9.0 and 10.0. A high value of optimal pH is a characteristic property of plant tyrosine aminotransferases (De-Eknamkul and Ellis 1987a). Therefore, plant aromatic aminotransferases are usually assayed in this range of pH values. Since the highest activity was observed with Tris–HCl buffer at pH 9.0, this was chosen for enzymatic assays to determine apparent kinetic parameters.

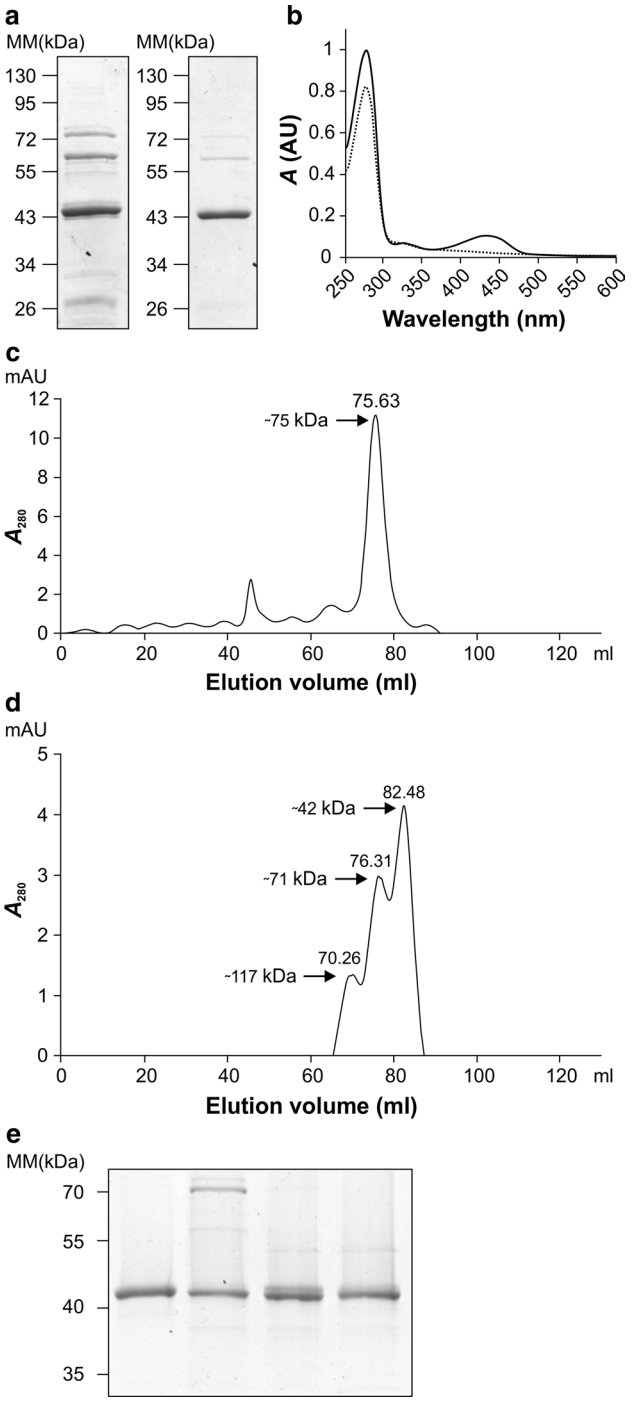

Fig. 2 Physical and spectral properties of recombinant EsAroAT1 and EsAroAT2. SDS-PAGE of affinity-purified EsAroAT1 (**a**, *left panel*) and EsAroAT2 (**a**, *right panel*). These preparations were used to acquire UV–visible absorption spectra (**b**). The characteristic peak for bound pyridoxal 5′-phosphate at 433 nm was observed for EsAroAT1 (*solid line*) but not for EsAroAT2 (*dashed line*). The same preparations were subjected to size-exclusion chromatography on a Superdex 200 column. Elution profile of EsAroAT1 (**c**) had a major peak corresponding to a homodimer (*first lane*, **e**). Three peaks were observed for EsAroAT2 (**d**) corresponding likely to a heterodimer with chaperone DnaK of ca. 68 kDa, a common host protein co-purified with heterologous recombinant proteins from *E. coli* (*lane 2*, **e**), a homodimer (*lane 3*) and a monomer (*lane 4*)

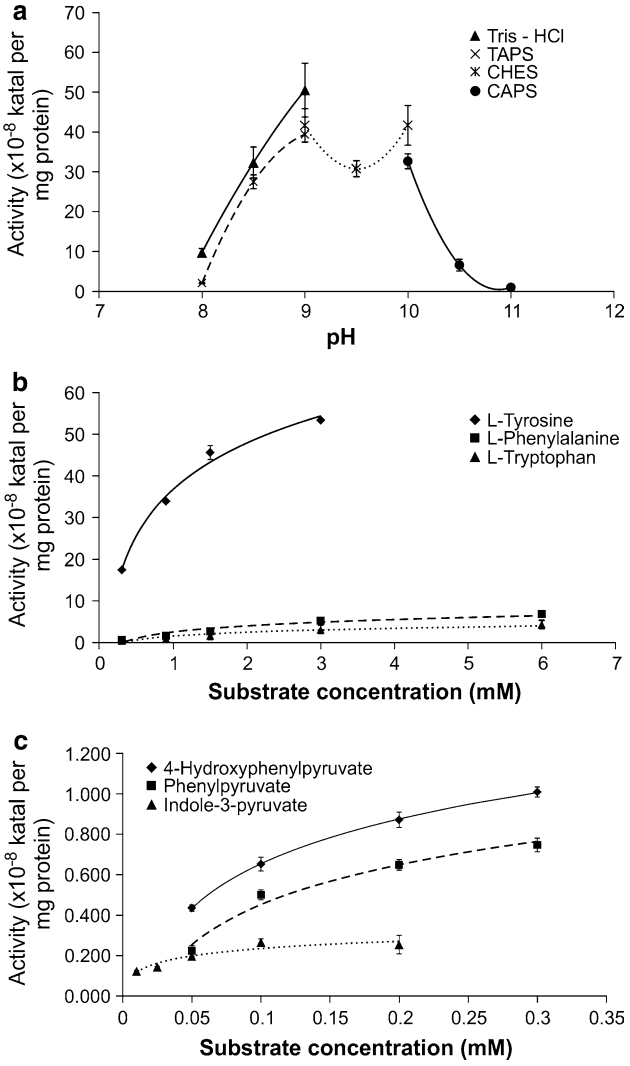

Fig. 3 EsAroAT1 enzymatic activity. **a** pH optima of purified recombinant EsAroAT1. Forward tyrosine aminotransferase activity assays were performed for 30 min at 30 °C in 100 mM of each buffer (Tris–HCl, TAPS, CHES and CAPS) at the indicated pH values in the presence of 0.05 μg of purified enzyme, 3 mM L-tyrosine (**5**), 1 mM α-ketoglutarate (**2**) and 0.1 mM EDTA. Steady-state enzyme kinetics of the forward (**b**) and reverse (**c**) reactions of purified recombinant EsAroAT1. Values represent the average specific and *error bars* represent standard deviation ($n = 3$)

Plots of catalytic activity versus substrate concentration for the forward and reverse aromatic aminotransferase reactions with α-ketoglutarate as amino group acceptor or L-glutamic acid as amino group donor, respectively, are compared in Fig. 3b, c. EsAroAT1 had the highest catalytic activity with L-tyrosine as substrate in the forward direction. In the reverse direction, phenylpyruvate and 4-hydroxyphenylpyruvate produced the highest activity. The catalytic activity in the forward reaction with tyrosine was higher than for the reverse reaction, by ca. 50-fold. Since it was recently reported that a cytosolic tyrosine

Table 3 EsAroAT1 kinetic parameters for forward aromatic aminotransferase reactions

Substrate	Cosubstrate	K_m (mM)	V_{max} ($\times 10^{-8}$ katal mg^{-1})	k_{cat} (s^{-1})	k_{cat}/K_m (mM^{-1} s^{-1})
L-Tyrosine	α-Ketoglutarate (1 mM)	0.91 ± 0.04	70.3 ± 1.8	32.8 ± 0.8	36.1 ± 0.8
L-Phenylalanine	α-Ketoglutarate (1 mM)	8.67 ± 1.21	18.0 ± 1.8	8.39 ± 0.82	0.972 ± 0.043
L-Tryptophan	α-Ketoglutarate (1 mM)	5.37 ± 1.04	7.56 ± 0.37	3.53 ± 0.17	0.672 ± 0.111
L-Tyrosine	Phenylpyruvate (1 mM)	0.698 ± 0.054	0.239 ± 0.003	0.112 ± 0.002	0.161 ± 0.011
L-Tyrosine	α-Ketomethylthiobutyrate (1 mM)	0.372 ± 0.011	5.90 ± 0.14	2.76 ± 0.06	7.41 ± 0.05
L-Tyrosine	Oxaloacetate (1 mM)	0.271 ± 0.021	1.73 ± 0.06	0.807 ± 0.029	2.99 ± 0.19
L-Tyrosine	Pyruvate (1 mM)	0.258 ± 0.026	0.543 ± 0.021	0.254 ± 0.010	0.988 ± 0.060
LSD		1.06	1.69	0.793	0.523
α-Ketoglutarate	L-Tyrosine (3 mM)	0.80 ± 0.04	70.0 ± 3.6	32.6 ± 1.7	40.8 ± 0.1

LSD Fisher's protected least significant difference at $p < 0.05$

Table 4 EsAroAT1 kinetic parameters for reverse aromatic aminotransferase reactions

Substrate	Cosubstrate	K_m (mM)	V_{max} ($\times 10^{-8}$ katal mg^{-1})	k_{cat} (s^{-1})	k_{cat}/K_m (mM^{-1} s^{-1})
Hydroxyphenylpyruvate	L-glutamate (10 mM)	0.105 ± 0.018	1.34 ± 0.08	0.627 ± 0.039	6.06 ± 0.930
Phenylpyruvate	L-glutamate (10 mM)	0.115 ± 0.006	1.76 ± 0.11	0.823 ± 0.50	7.18 ± 0.46
Indole-3-pyruvate	L-glutamate (10 mM)	0.037 ± 0.009	0.357 ± 0.063	0.166 ± 0.029	4.51 ± 0.432
Hydroxyphenylpyruvate	L-phenylalanine (10 mM)	0.311 ± 0.024	0.092 ± 0.004	0.043 ± 0.002	0.139 ± 0.008
LSD		0.0303	0.140	0.0660	1.06
L-glutamate	Phenylpyruvate (1 mM)	9.44 ± 0.31	1.73 ± 0.13	0.810 ± 0.061	0.0858 ± 0.0070

aminotransferase is involved in L-phenylalanine biosynthesis in petunia (Yoo et al. 2013), and that a phenylalanine :hydroxyphenylpyruvate aminotransferase (Ab-ArAT4) is required for the biosynthesis of tropane alkaloids in *Atropa belladonna* (Bedewitz et al. 2014), the corresponding reactions were tested. The capacity of different organic acids to substitute for α-ketoglutarate in the tyrosine aminotransferase reaction was also evaluated. Apparent kinetic parameters were determined using Lineweaver–Burk (double reciprocal) plots to analyze the Michaelis–Menten equation. Tables 3 and 4 present the kinetic parameters for the forward and reverse aromatic aminotransferase reactions, respectively. In the forward direction with α-ketoglutarate as acceptor substrate, the catabolism of L-tyrosine was clearly the preferred reaction as it produced the highest catalytic efficiency (k_{cat}/K_m) and reaction rate (V_{max}). In the reverse direction with L-glutamate as amino group donor, the catalytic efficiencies were relatively similar for the three aromatic aminotransferase reactions. Interestingly, the K_m values for the three organic acceptors using L-glutamate as co-substrate were lower than that for L-tyrosine in the forward direction. The K_m value for indole-3-pyruvate was particularly low, being in the mid-micromolar range (Table 4; Fig. 3b). Catalytic activity with L-tyrosine and phenylpyruvate was low, with a ca. 300-fold lower V_{max} value and a ca. 200-fold lower value of catalytic efficiency (k_{cat}/K_m) as compared with the preferred substrates L-tyrosine and α-ketoglutarate. Similarly, for the reverse reaction with hydroxyphenylpyruvate and L-phenylalanine, the catalytic activity was lower than with hydroxyphenylpyruvate and L-glutamate, with a ca. 14-fold reduced V_{max} value and a ca. 40-fold reduced value of catalytic efficiency. When tested with L-tyrosine as the variable substrate and a similar concentration of organic acid acceptor, the highest V_{max} value was observed with α-ketoglutarate, followed by α-ketomethylthiobutyrate, oxaloacetate, pyruvate and phenylpyruvate.

Discussion

Aromatic aminotransferases (EC 2.6.1.57) catalyze reactions using L-phenylalanine, L-tyrosine and L-tryptophan as amino donors and typically use α-ketoglutarate as the preferred amino acceptor in the forward direction (Fig. 1). In the reverse direction, L-glutamate is typically the preferred amino donor and keto acid derivatives of the aforementioned aromatic amino acids are amino acceptors. The present results indicate that EsAroAT1 is most similar to previously characterized tyrosine aminotransferases. Two Arabidopsis genes have been shown to encode catalytically active tyrosine aminotransferases having TAIR accession numbers At5g53970 (TAT7) (Holländer-Czytko et al. 2005; Riewe et al. 2012), and At5g36160 (Prabhu

and Hudson 2010). Analysis of a T-DNA insertion mutant for *TAT7* revealed a role in the utilization of tyrosine for the biosynthesis of tocopherols (Riewe et al. 2012). Both tocopherols and plastoquinone, a co-factor of phytoene desaturase involved in carotenoid biosynthesis, are derived from the prenylquinone pathway (DellaPenna and Pogson 2006). In this pathway, tyrosine aminotransferase provides 4-hydroxyphenylpyruvate to hydroxyphenylpyruvate dehydrogenase which forms the common metabolic precursor, homogentisate. Based on the crucial role of carotenoids in protection against photooxidative damage (Lichtenthaler 2007), the reaction catalyzed by tyrosine aminotransferase would be assumed to be essential for plant survival. Indeed, tyrosine aminotransferase was shown to be targeted by the herbicides cynmethylin and 5-benzyloxymethyl-1, 2 isoxazolines substituted with methylthiophene (methiozolin) or pyridine (Grossmann et al. 2012). Not only was the transamination of L-tyrosine being blocked in vivo, recombinant TAT7 was also inhibited in vitro by these chemicals. Transgenics expressing a yeast prephenate dehydrogenase, to by-pass tyrosine aminotransferase, exhibited tolerance to one of these herbicides. Another tyrosine aminotransferase was recently characterized from the opium poppy, *Papaver somniferum*, with a role in benzylisoquinoline alkaloid biosynthesis (Lee and Facchini 2011). Virus induced gene silencing resulted in reduced levels of benzylisoquinoline alkaloids, supporting the hypothesis that, like for TAT7, the enzyme may function as a tyrosine aminotransferase providing metabolic precursors for alkaloid biosynthesis. Similarly, tyrosine aminotransferase has been implicated in the biosynthesis of precursors for the formation of the secondary metabolite rosmarinic acid in *Anchusa officinalis* (De-Eknamkul and Ellis 1987b). As in the present study, Riewe et al. (2012) reported a higher V_{max} value of Arabidopsis TAT7 for the forward reaction with L-tyrosine and α-ketoglutarate versus the reverse reaction with 4-hydroxyphenylpyruvate and L-glutamate, by ca. 25-fold. However, the value of k_{cat} reported here for the forward reaction with L-tyrosine and α-ketoglutarate is higher than those previously reported for plant tyrosine aminotransferases, by ca. 10–100 fold (Riewe et al. 2012; Lee and Facchini 2011; Prabhu and Hudson 2010; Yoo et al. 2013). The kinetic parameters reported for the forward reactions are similar to those determined for mouse tyrosine aminotransferase (Mehere et al. 2010). Among plant aromatic aminotransferases, only the recently characterized phenylalanine:hyd roxyphenylpyruvate aminotransferase from *Atropa belladonna* has similar kinetic parameters as EsAroAT1, with a k_{cat}/K_m value of 87.2 mM^{-1} s^{-1} with 4-hydroxyphenylpyruvate and L-phenylalanine as substrates (Bedewitz et al. 2014).

In plants, L-phenylalanine biosynthesis can occur predominantly via the arogenate pathway, whereby prephenate is transaminated to arogenate, which is converted to L-phenylalanine by arogenate dehydratase (Maeda and Dudareva 2012; Tohge et al. 2013; Maeda et al. 2010; Cho et al. 2007; Corea et al. 2012). In an alternative pathway, prephenate is converted to phenylpyruvate by prephenate dehydratase, and phenylpyruvate is transaminated to L-phenylalanine. In transgenic Arabidopsis expressing a bacterial bifunctional chorismate mutase/prephenate dehydratase, this pathway appeared to be stimulated (Tzin et al. 2009). The occurrence of this alternative pathway in plants is supported by the functional complementation of the yeast prephenate dehydratase *pha2* mutant by selected Arabidopsis arogenate dehydratase genes (Bross et al. 2011). Recent evidence implicates a phenylpyruvate aminotransferase using L-tyrosine as an amino group donor to form L-phenylalanine (Yoo et al. 2013). The present data indicate that, unlike this tyrosine:phenylpyruvate aminotransferase and the phenylalanine:hydroxyphenylpyruvate aminotransferase from *Atropa belladonna* (Ab-ArAT4), EsAroAT1 has very low catalytic activity with a pair of aromatic substrates.

When assaying different organic acid acceptors at the same concentration, using L-tyrosine as the variable substrate, the second highest V_{max} value after that with α-ketoglutarate was observed with α-ketomethylthiobutyrate. This compound is an intermediate in the L-methionine salvage pathway. In mammals, it is transaminated to L-methionine by glutamine transaminases K and L [E.C. 2.6.1.–] (Cooper 2004; Pinto et al. 2014). Recent research has identified the corresponding gene and enzyme in *Bacillus subtilis* and tomato and maize, whose activity is coupled with an ω-amidase, hydrolyzing α-ketoglutaramate produced in the reaction (Zhang and Marsolais 2014; Ellens et al. 2014). Knockout mutants of glutamine transaminase K in *B. subtilis* are viable, suggesting that other aminotransferases may substitute for its function. In *Klebsiella pneumoniae*, tyrosine aminotransferase is involved in the transamination of α-ketomethylthiobutyrate (Heilbronn et al. 1999). The present data indicate that plant tyrosine aminotransferases may share the capacity to transaminate this substrate.

According to the present results, EsAroAT1 is most likely to function as a tyrosine aminotransferase in the prenylquinone pathway, an essential enzyme in higher plants (Riewe et al. 2012; Grossmann et al. 2012). EsAroAT1 is unlikely to contribute to ephedrine alkaloid biosynthesis through the catabolism of L-phenylalanine to phenylpyruvate as a precursor to benzaldehyde, since the K_m value for L-phenylalanine was nearly tenfold higher than that for L-tyrosine with α-ketoglutarate as co-substrate. Neither is EsAroAT1 likely to provide L-phenylalanine as a precursor to ephedrine alkaloids by acting as a phenylpyruvate aminotransferase. Although L-phenylalanine formation

represents its preferred reverse reaction, the enzyme has a clear preference for the forward reaction with L-tyrosine. In addition, L-tyrosine is implicated as the amino group donor in L-phenylalanine biosynthesis, at least in dicotyledonous plants (Yoo et al. 2013).

The lack of requirement for exogenous pyridoxal 5′-phosphate has been reported for numerous plant aromatic aminotransferases, for example by Gonda et al. (2010), Prabhu and Hudson (2010), Hirata et al. (2012), and Lee and Facchini (2011) and references therein. The reason for the lack of co-purification of EsAroAT2 with its co-factor, pyridoxal 5′-phosphate, is not obvious. In the crystal structure of human tyrosine aminotransferase (PDB ID 3DYD), the co-factor binding site, including the conserved arginine interacting with the phosphate group, corresponding to Arg^{288} in mouse tyrosine aminotransferase (Mehere et al. 2010), is very close to the dimer interface. It is therefore possible that the lack of co-factor may result in a weaker dimer, hence the different molecular forms of EsAroAT2. Alternatively, the absence of the co-factor may have global effects of the structure of the protein.

In conclusion, a highly active tyrosine aminotransferase, EsAroAT1, was characterized from *E. sinica*. Although they were logical candidates, neither EsAroAT1 nor EsAroAT2 had catalytic activity with the ephedrine alkaloid precursors, phenylpropanedione or *S*-phenylacetylcarbinol. Future studies investigating ephedrine alkaloid biosynthesis will benefit greatly from access to an *E. sinica* EST database developed in this study. This resource is instrumental to the discovery of genes involved in the biosynthetic pathway. In the long term, the availability of cloned enzymes of ephedrine alkaloid biosynthesis may allow the development of synthetic biology platforms for the synthesis of amphetamine analogs with known or novel pharmaceutical properties.

Acknowledgments This research was supported by Research Grant No. CA-9117-09 from the Canada-Israel Binational Agricultural Research and Development Fund, the Natural Sciences and Engineering Research Council and Agriculture and Agri-Food Canada to E.L., P.F. and F.M. Granting agencies were not involved in study design; in the collection, analysis and interpretation of data; in the writing of the report; and in the decision to submit the article for publication. K.K. was co-supervised by Norman Hüner during his M. Sc. program (Department of Biology, University of Western Ontario). We thank staff at the London Development and Research Centre, Agriculture and Agri-Food Canada, Tim McDowell for assistance with GC–MS, Sudhakar Pandurangan with RT-quantitative PCR, and Alex Molnar for the preparation of figures. We acknowledge support from the Genome Canada PhytoMetaSyn project for bioinformatic analysis.

Compliance with ethical standards

Conflict of interest The authors declare that they have no conflict of interest.

References

Bedewitz MA, Gongora-Castillo E, Uebler JB, Gonzales-Vigil E, Wiegert-Rininger KE, Childs KL, Hamilton JP, Vaillancourt B, Yeo YS, Chappell J, DellaPenna D, Jones AD, Buell CR, Barry CS (2014) A root-expressed L-phenylalanine:4-hydroxyphenylpyruvate aminotransferase is required for tropane alkaloid biosynthesis in *Atropa belladonna*. Plant Cell 26:3745–3762. doi:10.1105/tpc.114.130534

Bensky D, Gamble A, Kaptchuk T (1986) Chinese Herbal Medicine. Materia Medica, Eastland, Seattle, Washington

Bolanos-Garcia VM, Davies OR (2006) Structural analysis and classification of native proteins from *E. coli* commonly co-purified by immobilised metal affinity chromatography. Biochim Biophys Acta 1760:1304–1313. doi:10.1016/j.bbagen.2006.03.027

Bross CD, Corea ORA, Kaldis A, Menassa R, Bernards MA, Kohalmi SE (2011) Complementation of the *pha2* yeast mutant suggests functional differences for arogenate dehydratases from *Arabidopsis thaliana*. Plant Physiol Biochem 49:882–890. doi:10.1016/j.plaphy.2011.02.010

Bruneton J (1995) Pharmacognosy, phytochemistry. Medicinal Plants. Intercept Ltd., Hampshire

Cho MH, Corea ORA, Yang H, Bedgar DL, Laskar DD, Anterola AM, Moog-Anterola FA, Hood RL, Kohalmi SE, Bernards MA, Kang C, Davin LB, Lewis NG (2007) Phenylalanine biosynthesis in *Arabidopsis thaliana*—identification and characterization of arogenate dehydratases. J Biol Chem 282:30827–30835. doi:10.1074/jbc.M702662200

Collier RH, Kohlhaw G (1972) Nonidentity of aspartate and aromatic aminotransferase components of transaminase-a in *Escherichia-coli*. J Bacteriol 112:365–371

Cooper AJ (2004) The role of glutamine transaminase K (GTK) in sulfur and α-keto acid metabolism in the brain, and in the possible bioactivation of neurotoxicants. Neurochem Int 44:557–577. doi:10.1016/j.neuint.2003.12.002

Corea ORA, Ki C, Cardenas CL, Kim S-J, Brewer SE, Patten AM, Davin LB, Lewis NG (2012) Arogenate dehydratase isoenzymes profoundly and differentially modulate carbon flux into lignins. J Biol Chem 287:11446–11459. doi:10.1074/jbc.M111.322164

Dal Cin V, Tieman DM, Tohge T, McQuinn R, de Vos RC, Osorio S, Schmelz EA, Taylor MG, Smits-Kroon MT, Schuurink RC, Haring MA, Giovannoni J, Fernie AR, Klee HJ (2011) Identification of genes in the phenylalanine metabolic pathway by ectopic expression of a MYB transcription factor in tomato fruit. Plant Cell 23:2738–2753. doi:10.1105/tpc.111.086975

de la Torre F, De Santis L, Suarez MF, Crespillo R, Cánovas FM (2006) Identification and functional analysis of a prokaryotic-type aspartate aminotransferase: implications for plant amino acid metabolism. Plant J 46:414–425. doi:10.1111/j.1365-313X.2006.02713.x

de la Torre FN, El-Azaz J, Ávila C, Cánovas FM (2014) Deciphering the role of aspartate and prephenate aminotransferase activities in plastid nitrogen metabolism. Plant Physiol 164:92–104. doi:10.1104/pp.113.232462

De-Eknamkul W, Ellis BE (1987a) Purification and characterization of tyrosine aminotransferase activities from *Anchusa officinalis* cell cultures. Arch Biochem Biophys 257:430–438

De-Eknamkul W, Ellis BE (1987b) Tyrosine aminotransferase: the entrypoint enzyme of the tyrosine-derived pathway in rosmarinic acid biosynthesis. Phytochemistry 26:1941–1946

DellaPenna D, Pogson BJ (2006) Vitamin synthesis in plants: tocopherols and carotenoids. Annu Rev Plant Biol 57:711–738. doi:10.1146/annurev.arplant.56.032604.144301

Ellens KW, Richardson LG, Frelin O, Collins J, Ribeiro CL, Hsieh YF, Mullen RT, Hanson AD (2014) Evidence that glutamine

transaminase and omega-amidase potentially act in tandem to close the methionine salvage cycle in bacteria and plants. Phytochemistry 113:160–169. doi:10.1016/j.phytochem.2014.04.012

Finn RD, Bateman A, Clements J, Coggill P, Eberhardt RY, Eddy SR, Heger A, Hetherington K, Holm L, Mistry J, Sonnhammer EL, Tate J, Punta M (2014) Pfam: the protein families database. Nucleic Acids Res 42:D222–D230. doi:10.1093/nar/gkt1223

Givan CV (1980) Aminotransferases in higher plants. In: Miflin BJ (ed) Amino acids and derivatives, vol 5. The biochemistry of plantsAcademic Press, New York, pp 329–357

Gonda I, Bar E, Portnoy V, Lev S, Burger J, Schaffer AA, Tadmor Y, Gepstein S, Giovannoni JJ, Katzir N, Lewinsohn E (2010) Branched-chain and aromatic amino acid catabolism into aroma volatiles in *Cucumis melo* L. fruit. J Exp Bot 61:1111–1123. doi:10.1093/jxb/erp390

Graindorge M, Giustini C, Jacomin AC, Kraut A, Curien G, Matringe M (2010) Identification of a plant gene encoding glutamate/aspartate-prephenate aminotransferase: the last homeless enzyme of aromatic amino acids biosynthesis. FEBS Lett 584:4357–4360. doi:10.1016/j.febslet.2010.09.037

Grossmann K, Hutzler J, Tresch S, Christiansen N, Looser R, Ehrhardt T (2012) On the mode of action of the herbicides cinmethylin and 5-benzyloxymethyl-1, 2-isoxazolines: putative inhibitors of plant tyrosine aminotransferase. Pest Manag Sci 68:482–492. doi:10.1002/ps.2319

Groves RA, Hagel JM, Zhang Y, Kilpatrick K, Levy A, Marsolais F, Lewinsohn E, Sensen CW, Facchini PJ (2015) Transcriptome profiling of khat (*Catha edulis*) and *Ephedra sinica* reveals gene candidates potentially involved in amphetamine-type alkaloid biosynthesis. PLoS One 10:e0119701. doi:10.1371/journal.pone.0119701

Grue-Sørensen G, Spenser ID (1994) Biosynthetic route to the *Ephedra* alkaloids. J Am Chem Soc 116:6195–6200

Hagel JM, Krizevski R, Kilpatrick K, Sitrit Y, Marsolais F, Lewinsohn E, Facchini PJ (2011) Expressed sequence tag analysis of khat (*Catha edulis*) provides a putative molecular biochemical basis for the biosynthesis of phenylpropylamino alkaloids. Genet Mol Biol 34:640–646. doi:10.1590/S1415-47572011000400017

Hagel JM, Krizevski R, Marsolais F, Lewinsohn E, Facchini PJ (2012) Biosynthesis of amphetamine analogs in plants. Trends Plant Sci 17:404–412. doi:10.1016/j.tplants.2012.03.004

Haller CA, Benowitz NL (2000) Adverse cardiovascular and central nervous system events associated with dietary supplements containing *Ephedra* alkaloids. N Engl J Med 343:1833–1838. doi:10.1056/nejm200012213432502

Heilbronn J, Wilson J, Berger BJ (1999) Tyrosine aminotransferase catalyzes the final step of methionine recycling in *Klebsiella pneumoniae*. J Bacteriol 181:1739–1747

Hirata H, Ohnishi T, Ishida H, Tomida K, Sakai M, Hara M, Watanabe N (2012) Functional characterization of aromatic amino acid aminotransferase involved in 2-phenylethanol biosynthesis in isolated rose petal protoplasts. J Plant Physiol 169:444–451. doi:10.1016/j.jplph.2011.12.005

Hirotsu K, Goto M, Okamoto A, Miyahara I (2005) Dual substrate recognition of aminotransferases. Chem Rec 5:160–172. doi:10.1002/tcr.20042

Holländer-Czytko H, Grabowski J, Sandorf I, Weckermann K, Weiler EW (2005) Tocopherol content and activities of tyrosine aminotransferase and cystine lyase in *Arabidopsis* under stress conditions. J Plant Physiol 162:767–770. doi:10.1016/j.jplph.2005.04.019

Howell JM, Winstone TL, Coorssen JR, Turner RJ (2006) An evaluation of in vitro protein-protein interaction techniques: assessing contaminating background proteins. Proteomics 6:2050–2069. doi:10.1002/pmic.200500517

Ishikawa K, Kaneko E, Ichiyama A (1996) Pyridoxal 5′-phosphate binding of a recombinant rat serine:pyruvate/alanine:glyoxylate aminotransferase. J Biochem 119:970–978

Krizevski R, Bar E, Shalit O, Sitrit Y, Ben-Shabat S, Lewinsohn E (2010) Composition and stereochemistry of ephedrine alkaloids accumulation in *Ephedra sinica* Stapf. Phytochemistry 71:895–903. doi:10.1016/j.phytochem.2010.03.019

Krizevski R, Bar E, Shalit OR, Levy A, Hagel JM, Kilpatrick K, Marsolais F, Facchini PJ, Ben-Shabat S, Sitrit Y, Lewinsohn E (2012) Benzaldehyde is a precursor of phenylpropylamino alkaloids as revealed by targeted metabolic profiling and comparative biochemical analyses in *Ephedra* spp. Phytochemistry 81:71–79. doi:10.1016/j.phytochem.2012.05.018

Lee E-J, Facchini PJ (2011) Tyrosine aminotransferase contributes to benzylisoquinoline alkaloid biosynthesis in opium poppy. Plant Physiol 157:1067–1078. doi:10.1104/pp.111.185512

Leete E (1958) Biogenesis of D-norpseudo ephedrine in *Catha-edulis*. Chem Ind 1088–1089

Lewis WH, Elvin-Lewis MPF (1977) Medical botany, plants affecting man's health. Wiley Interscience, USA

Lichtenthaler H (2007) Biosynthesis, accumulation and emission of carotenoids, α-tocopherol, plastoquinone, and isoprene in leaves under high photosynthetic irradiance. Photosynth Res 92:163–179. doi:10.1007/s11120-007-9204-y

Liepman AH, Olsen LI (2004) Genomic analysis of aminotransferases in *Arabidopsis thaliana*. Crit Rev Plant Sci 23:73–89. doi:10.1080/07352680490273419

Maeda H, Dudareva N (2012) The shikimate pathway and aromatic amino acid biosynthesis in plants. Annu Rev Plant Biol 63:73–105. doi:10.1146/annurev-arplant-042811-105439

Maeda H, Shasany AK, Schnepp J, Orlova I, Taguchi G, Cooper BR, Rhodes D, Pichersky E, Dudareva N (2010) RNAi suppression of arogenate dehydratase1 reveals that phenylalanine is synthesized predominantly via the arogenate pathway in petunia petals. Plant Cell 22:832–849. doi:10.1105/tpc.109.073247

Maeda H, Yoo H, Dudareva N (2011) Prephenate aminotransferase directs plant phenylalanine biosynthesis via arogenate. Nat Chem Biol 7:19–21. doi:10.1038/nchembio.485

Mehere P, Han Q, Lemkul JA, Vavricka CJ, Robinson H, Bevan DR, Li J (2010) Tyrosine aminotransferase: biochemical and structural properties and molecular dynamics simulations. Protein Cell 1:1023–1032. doi:10.1007/s13238-010-0128-5

Mehta PK, Hale TI, Christen P (1993) Aminotransferases - Demonstration of homology and division into evolutionary subgroups. Eur J Biochem 214:549–561. doi:10.1111/j.1432-1033.1993.tb17953.x

Nierop Groot MN, de Bont JA (1999) Involvement of manganese in conversion of phenylalanine to benzaldehyde by lactic acid bacteria. Appl Environ Microbiol 65:5590–5593

Okada T, Mikage M, Sekita S (2008) Molecular characterization of the phenylalanine ammonia-lyase from *Ephedra sinica*. Biol Pharm Bull 31:2194–2199

Pinto JT, Krasnikov BF, Alcutt S, Jones ME, Dorai T, Villar MT, Artigues A, Li J, Cooper AJL (2014) Kynurenine aminotransferase III and glutamine transaminase L are identical enzymes that have cysteine *S*-conjugate β-lyase activity and can transaminate L-selenomethionine. J Biol Chem 289:30950–30961. doi:10.1074/jbc.M114.591461

Prabhu PR, Hudson AO (2010) Identification and partial characterization of an L-tyrosine aminotransferase (TAT) from *Arabidopsis thaliana*. Biochem Res Int 2010:549572

Riewe D, Koohi M, Lisec J, Pfeiffer M, Lippmann R, Schmeichel J, Willmitzer L, Altmann T (2012) A tyrosine aminotransferase involved in tocopherol synthesis in *Arabidopsis*. Plant J 71:850–859. doi:10.1111/j.1365-313X.2012.05035.x

Rothman RB, Vu N, Partilla JS, Roth BL, Hufeisen SJ, Compton-Toth BA, Birkes J, Young R, Glennon RA (2003) In vitro characterization of ephedrine-related stereoisomers at biogenic amine transporters and the receptorome reveals selective actions as norepinephrine transporter substrates. J Pharmacol Exp Ther 307:138–145. doi:10.1124/jpet.103.053975

Rudat J, Brucher BR, Syldatk C (2012) Transaminases for the synthesis of enantiopure beta-amino acids. AMB Express 2:11. doi:10.1186/2191-0855-2-11

Schneider G, Kack H, Lindqvist Y (2000) The manifold of vitamin B6 dependent enzymes. Structure 8:R1–R6

Tohge T, Watanabe M, Hoefgen R, Fernie AR (2013) Shikimate and phenylalanine biosynthesis in the green lineage. Front Plant Sci 4:62. doi:10.3389/fpls.2013.00062

Tzin V, Malitsky S, Aharoni A, Galili G (2009) Expression of a bacterial bi-functional chorismate mutase/prephenate dehydratase modulates primary and secondary metabolism associated with aromatic amino acids in Arabidopsis. Plant J 60:156–167. doi:10.1111/j.1365-313X.2009.03945.x

Wang C-S, Vodkin L (1994) Extraction of RNA from tissues containing high levels of procyanidins that bind RNA. Plant Mol Biol Rep 12:132–145. doi:10.1007/bf02668374

Yamasaki K, Sankawa U, Shibata S (1969) Biosynthesis of ephedrine in *Ephedra*. Participation of C_6–C_1 unit. Tetrahedron Lett 10:4099–4102

Yoo H, Widhalm JR, Qian Y, Maeda H, Cooper BR, Jannasch AS, Gonda I, Lewinsohn E, Rhodes D, Dudareva N (2013) An alternative pathway contributes to phenylalanine biosynthesis in plants via a cytosolic tyrosine:phenylpyruvate aminotransferase. Nat Commun 4:2833. doi:10.1038/ncomms3833

Zerbino DR, Birney E (2008) Velvet: algorithms for *de novo* short read assembly using de Bruijn graphs. Genome Res 18:821–829. doi:10.1101/gr.074492.107

Zhang Q, Marsolais F (2014) Identification and characterization of omega-amidase as an enzyme metabolically linked to asparagine transamination in Arabidopsis. Phytochemistry 99:36–43. doi:10.1016/j.phytochem.2013.12.020